Available online at www.sciencedirect.com
SCIENCE DIRECT®
International Journal of Heat and Mass Transfer 47 (2004) 2183–2189
International Journal of HEAT and MASS TRANSFER
www.elsevier.com/locate/ijhmt

High heat flux removal from a single-side heated monoblock using flow boiling

Ronald D. Boyd *, Ali Ekhlassi, Penrose Cofie, Hongtao Zhang

Thermal Science Research Center, College of Engineering, P.O. Box 4208, Prairie View A&M University, Prairie View, TX 77446-4208, USA

Received 11 April 2003; received in revised form 22 November 2003

Abstract

The robust design of one-side-heated plasma-facing components and other high heat flux components is dependent on knowing the local distribution of inside wall heat flux in the flow channels. The local inside wall heat flux can be obtained from selectively chosen local plasma-facing component wall temperatures close to the inside boundary of the flow channel. To this end, three-dimensional thermal measurements for a one-side-heated monoblock were made and show: (1) the three-dimensional variation of the wall temperature close to both the heated and fluid/solid surface boundaries, (2) the resultant effects of mass velocity on the three-dimensional wall temperature/outside heat flux relationship, and (3) the occurrence of local critical heat flux and local post-critical heat flux. The monoblock has a 180.0 mm heated length, has a 10.0 mm inside diameter, and has a square cross-section with 30.0 mm nominal outside surfaces.
Published by Elsevier Ltd.

1. Introduction

In the development of plasma-facing components and high heat flux heat sinks (or components) for other applications, the components are usually subjected to a peripherally non-uniform heat flux. Even if the applied heat flux is uniform in the axial direction, both intuition and recent investigations have clearly shown that both the local heat flux and the eventual critical heat flux (CHF) in this three-dimensional case will differ significantly from similar quantities found in the voluminous body of data for uniformly heated flow channels. Although this latter case has been used in the past as an estimate for the former case, more study has become necessary to examine the three-dimensional temperature and heat flux distributions and related CHF.

The test section configuration under study for this work consists of a square cross-section monoblock with an inside circular 10.0 mm diameter coolant channel bored through the center. The outside square sides are 30.0 mm. The main section of the monoblock is 200.0 mm long. The monoblock is subjected to a constant heat flux on one side only. Water is the coolant. The inlet water temperature is held near 26.0 °C and the exit pressure is maintained at 0.207 MPa (T_{sat} = 121.3 °C). Thermocouples (0.5 mm OD, stainless steel sheathed, Type-J) were placed in 48 thermal well locations inside the solid Glidcop Copper monoblock. For each of four axial stations, three thermocouples were embedded at three radial and four circumferential locations (0°, 45°, 135° and 180°, where 0° corresponds to that portion of the axis of symmetry close to the heated surface). The mass velocity was 1.18 M g/m^2 s.

A detail description of the test facility, experimental, and measurement details are given elsewhere by Boyd et al. [1]. The flow parameter ranges for the present test facility are as follows: 0–25.0 M W/m^2 heat flux, 0–12.0 m/s velocity, 0.2–3.5 MPa inlet pressure, and

* Corresponding author. Tel.: +1-936-857-4811; fax: +1-936-857-4858.
E-mail address: ronald_boyd@pvamu.edu (R.D. Boyd).

0017-9310/$ - see front matter Published by Elsevier Ltd.
doi:10.1016/j.ijheatmasstransfer.2003.11.012

18–130.0 °C inlet temperature. The thermocouples were calibrated to within 0.1 °C with a precision calibrator.

International efforts are vigorously proceeding in the investigation of heat transfer and related CHF in one-side-heated flow channels. Some examples of recent one-side heating efforts include: (1) the international round-robin monoblock CHF swirl-flow tests by Youchison et al. [2]; (2) CHF in multiple square channels by Akiba et al. [3]; (3) CHF comparison of an attached-fin hypervapotron and porous coated surface by Youchison et al. [4]; (4) CHF enhancements due to wire inserts by Youchison et al. [5]; (5) post-CHF with and without swirl-flow in a monoblock by Marshall [6]; (6) CHF data base of JAERI by Boscary et al. [7,8]; (7) post-CHF enhancement factors by Marshall et al. [9]; (8) CHF peaking factor empirical correlations by Inasaka and Nariari [10], and Akiba et al. [11]; (9) CHF correlation modification to account for peripheral non-uniform heating by Celata et al. [12]; (10) comparison of one-side heating with uniform heating by Boyd [13]; (11) single- and two-phase subcooled flow boiling heat transfer in smooth and swirl tubes by Araki et al. [14]; (12) smooth tube heat transfer, CHF and post-CHF by Becker et al. [15]; (13) turbulent heat transfer analysis by Gärtner et al. [16]; and, (14) an extensive review on actively cooled plasma-facing components by Nygren [17].

2. Monoblock test section

The monoblock test sections were fabricated from Type AL-15 Glidcop Grade Copper. A detailed description of the monoblock test section is shown in Fig. 1. The overall length of the monoblock test section, including the inlet and outlet reduced diameter sections, is 328.0 mm. The main section of the monoblock test section (available for heating) is 200.0 mm long with a nominal outside surface width of the square cross-section monoblock of 30.0 mm and an inside diameter of 10.0 mm. For these tests, the actual directly heated length, L, was 180.0 mm. In Fig. 1, isometric and longitudinal side views are shown. The flow channel inlet and exit are indicated in the latter view. Also shown are four axial stations labeled A–A, B–B, C–C, and D–D, which are axial locations where thermocouple (TC) wells exist for local in-depth wall temperature measurements. The purpose of the four axial locations is to obtain an estimate of the axial distribution of the monoblock test section wall temperature for a given applied heat flux. Since the geometry of the TC wells is identical at all four primary axial stations, a detail description will be given for only one axial station. For example, the A–A axial station has 12 TC wells, with 10 wells in plane A1 and one each in planes A2 and A3 which are axially dis-

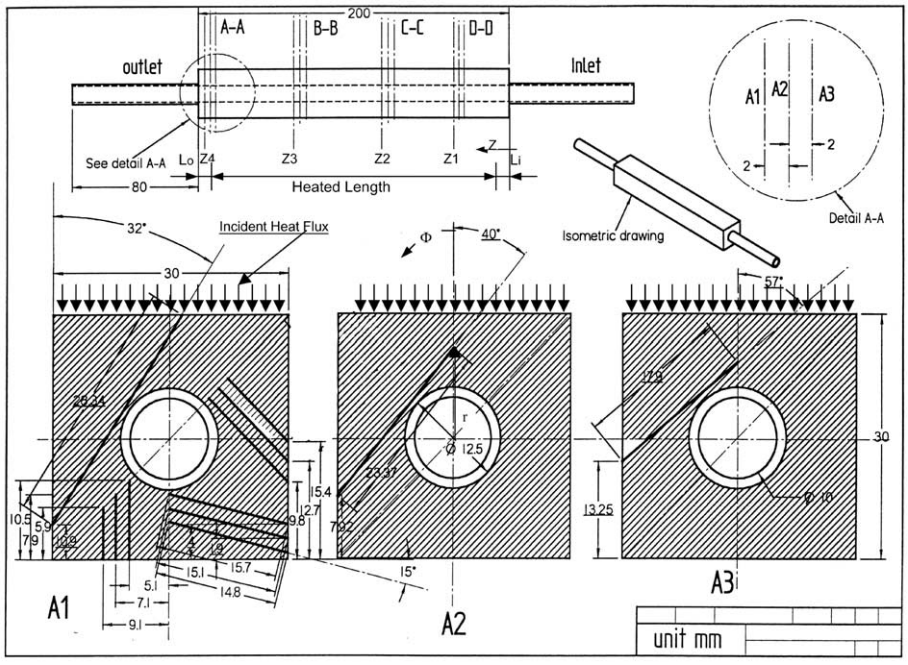

Fig. 1. Monoblock test section used for local temperature and heat transfer measurements. Water flows through the 10.0 mm diameter channel. The thermocouple (TC) wells are the solid black lines with specified lengths and angles. The outer concentric circle around the 10.0 mm inner diameter channel should not appear in the shown sections but has been added to show the outside diameter of the channel near the inlet and exit.

placed upstream from plane A1 by 2.0 and 4.0 mm, respectively.

The TCs at station A–A will give both radial and circumferential distributions of the local wall temperature. Hence, a combination of all axial stations will produce a three-dimensional distribution of the test section local wall temperature as a function of the applied heat flux and the water flow regime which will vary from single-phase at the test section inlet to subcooled pre- and post-CHF near the exit. The applied heat flux comes from a DC power supply which provides resistive heating to the test section via one, grade G-20 graphite flat heater which is placed over a 1.0 mm thick aluminum nitride layer which in turn rests on the monoblock test section shown in Fig. 1. As noted above, the power supply feeds the heater element (see Fig. 2) in the experimental set-up through a copper bus duct/cabling (bus bar) system [1].

3. Results

Design of robust plasma-facing components (PFCs) must be based on accurate three-dimensional conjugate flow boiling analyses and optimizations of the PFC local wall temperature, and hence on the local flow boiling regime variations. Such analyses must have three-dimensional data as a basis for comparison, assessment, and flow boiling correlation adaptation for localized boiling. As an initial part of an effort to begin to provide such data, selected steady-state results are presented for the above-noted conditions for the: (1) three-dimensional variations of the monoblock test section wall temperature as functions of the circumferential (ϕ), radial (r), and axial (Z) coordinates; (2) outside steady-state heat flux as a function of the local wall temperature; (3) occurrence of pre- and post local-CHF (local dry-out); and, (4) dependence of the above on mass velocity changes. The three-dimensional variations in the local wall temperature will be discussed first.

3.1. Three-dimensional variations

The circumferential variations in the channel wall temperature are presented in Fig. 3a and b for eight levels of the net, outside, single-side heat flux, q_o. Fig. 3a and b show such variations close to the outside (partially heated) boundary and the inside fluid/solid boundary, respectively. Comparing the two sets of plots, one observes two very different circumferential wall temperature variations near the two boundaries. Since there are only four circumferential locations for each set of measurements, these distributions will not show the exact local circumferential slopes but the quantitative trends at the four locations is evident. The locus of the data in Fig. 3a (near the outside partially heated boundary) displays approximately the correct boundary condition of a zero circumferential temperature gradient as ϕ approaches 180.0° but differs from the profile near the fluid/solid boundary. In Fig. 3b which shows the local circumferential monoblock wall temperature variation close to the fluid/solid boundary, the temperature is almost constant between $\phi = 45.0°$ and 135.0°. This is due to the relatively large thickness of the test section in some cases and due to localized boiling in other cases. For smaller TS thicknesses, the variation would be greater in regions where a phase change is not occurring. In the limit of ϕ approaching 180.0° in Fig. 3a and b, the wall temperature is well above the fluid temperature and increases as q_o increases.

Fig. 4 displays the radial temperature profiles at $\phi = 45.0°$ and shows small variations with respect to r and some values of ϕ. This is of course contrasted with larger radial variations as displayed by comparing Fig. 3a and b at for example, $\phi = 0°$.

Finally, Fig. 5 shows the remaining portion of the three-dimensional variations via the axial wall temperature profiles which include the four axial stations. For this work, the heater length (L) was 180.0 mm long (in the axial direction) and was placed asymmetrically on test section (200.0 mm long). More specifically, there was a 4.0 mm ($= L_o$) unheated portion (i.e. unheated directly) at the down-stream most part of the square monoblock test section; and, there was a 16.0 mm ($= L_i$) unheated portion (i.e. unheated directly) at the upstream most part of the monoblock test section. The curves shown in Fig. 5 are for test section locations along the axis of symmetry ($\phi = 0.0°$) and close the heated boundary.

3.2. Net incident heat flux/wall temperature relationship

Two cases are presented here which show the effects at two different levels of mass velocity on the relationship between the net incident (outside) monoblock heat flux (q_o) and the local wall temperature (T_w). Although not identical, this relationship between q_o and T_w would be directly related to the two-dimensional local boiling curve if the radius at which this relationship was considered was equal to the inside radius of the flow channel. This work will eventually lead to the latter. In Fig. 6, the steady-state incident heat flux/wall temperature relationship is presented: (1) for the axis of symmetry with $\phi = 0.0°$; (2) for axial locations of $Z = 143.1$, 145.1 and 147.1 mm (nominally, $Z = Z_3 = 147.1$ mm or cross-section B–B in Fig. 1); and, (3) for radii of 12.82, 10.62 and 7.95 mm, respectively.

These curves are complete in that they not only show the three flow regimes (partially nucleate boiling, fully developed flow boiling, and film boiling) but an apparent local critical heat flux and a post-CHF region (local film flow boiling). The occurrence of the local CHF is

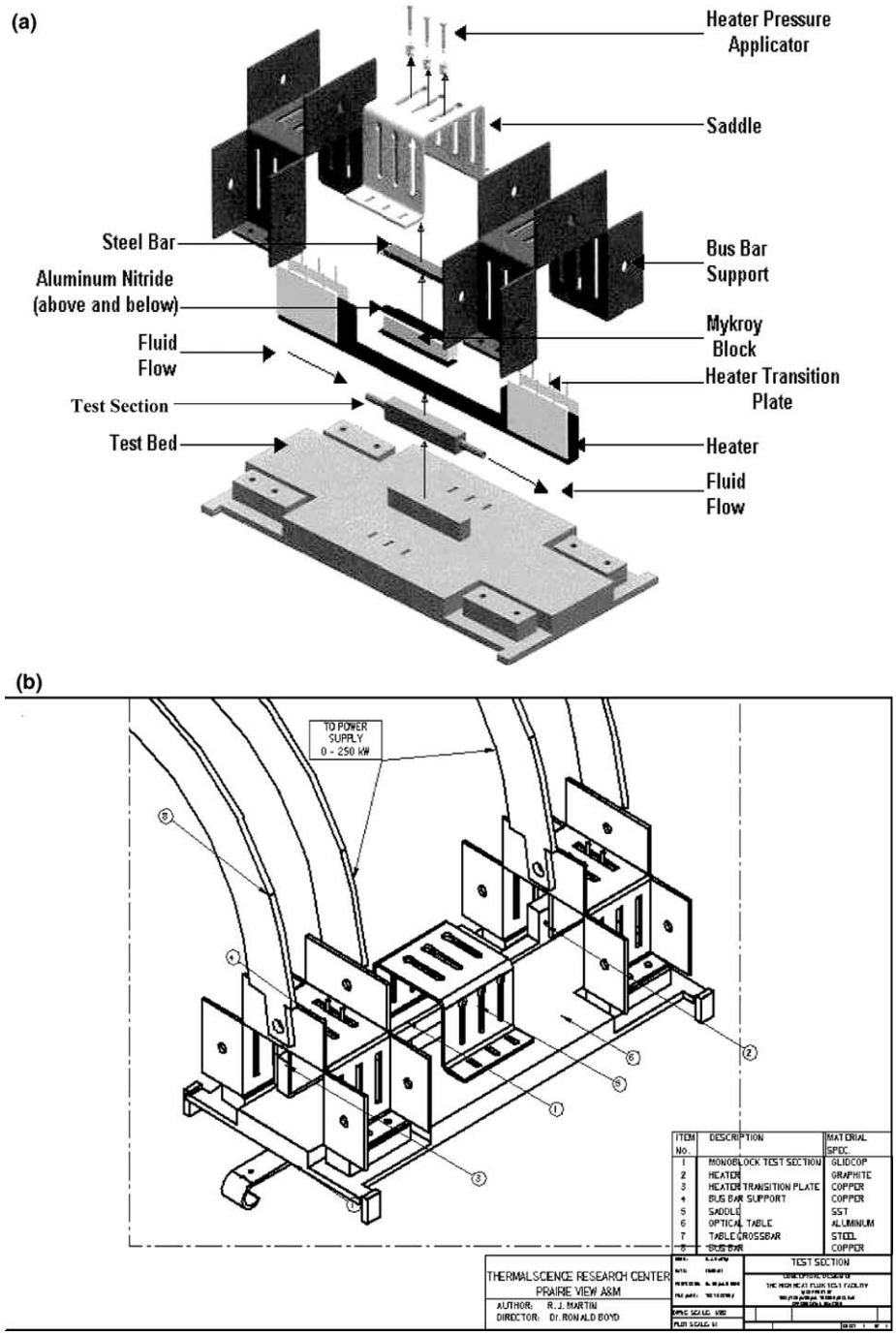

Fig. 2. (a) High heat flux monoblock test section expanded assembly. (b) Monoblock test section assembly with heater, flexible bus bars, and test bed (see Figs. 1 and 2a for component labeling and additional details).

denoted by a local decrease in the slopes of the curves after the slopes have become large. The normal temperature escalation, which accompanies CHF in uniformly heated tubes, is absent due to the single-side-heated flow channel geometry and the resulting three-dimensional conjugate heat transfer (which is absent in the uniformly heated cases). This escalation may occur when a global CHF is reached [2]. The reduction in the slope

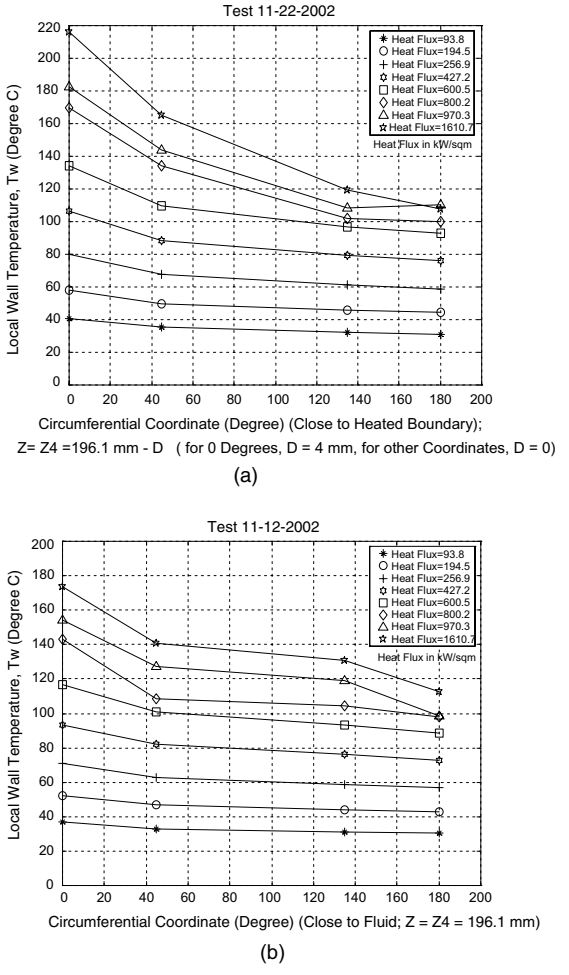

Fig. 3. (a) Circumferential monoblock wall temperature profile from the thermocouples nearest to the heated boundary (i.e., away from the fluid/solid boundary) as a function of the net incident heat flux at $Z = Z_4 = 196.1$ mm. (b) Circumferential monoblock wall temperature profile from the thermocouples nearest to the fluid/solid boundary as a function of net incident heat flux, at $Z = Z_4 = 196.1$ mm ($L_i = 16.0$ mm and $L_o = 4.0$ mm).

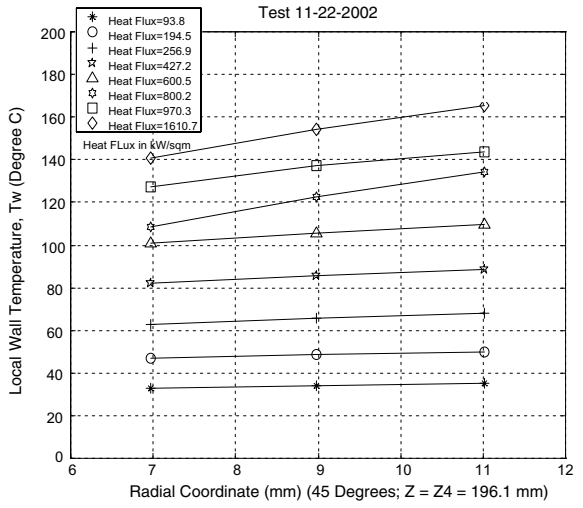

Fig. 4. Radial wall temperature profile for the monoblock flow channel at $\phi = 45.0°$ and $Z = Z_4 = 196.1$ mm as a function of the net incident heat flux ($L_i = 16.0$ mm and $L_o = 4.0$ mm).

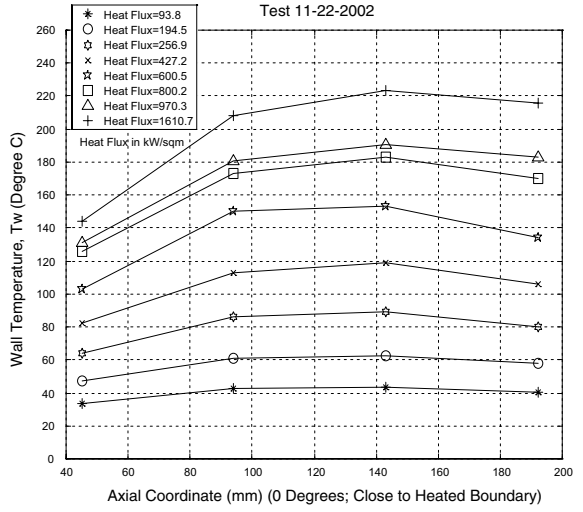

Fig. 5. Monoblock axial wall temperature profiles from the thermocouples at $\phi = 0.0°$ (close to the heated boundary) as a function of the net incident heat flux.

of each curve in Fig. 6 suggests a stable entry into the local post-CHF regime at $\phi = 0.0°$ and $Z = Z_3 = 147.1$ mm.

From Fig. 6, the local CHF (or local surface dry-out) occurred slightly above approximately 780.0 and 970.0 kW/m^2 for a mass velocity of 0.59 and 1.18 M g/m^2 s, respectively. Beyond these heat flux levels, the local slope of the incident heat flux/local wall temperature curve decreased, denoting the entry into a post-CHF or a locally stable film flow boiling regime.

In the regions where the slopes of the q_o vs. T_w curves attained an initial peak, one observes this peak slope increasing as the local radius decreases, i.e., as the fluid/solid boundary is approached. This region of peak slopes denotes a region of fully develop flow boiling existing locally at $\phi = 0°$ but not at much larger values of ϕ. Further, the data suggests that the fully-developed boiling region occurs at nearly the same local wall temperature for both velocities. This of course is exactly what the classical literature (e.g. see Collier [18]) has shown for uniformly heated tubes.

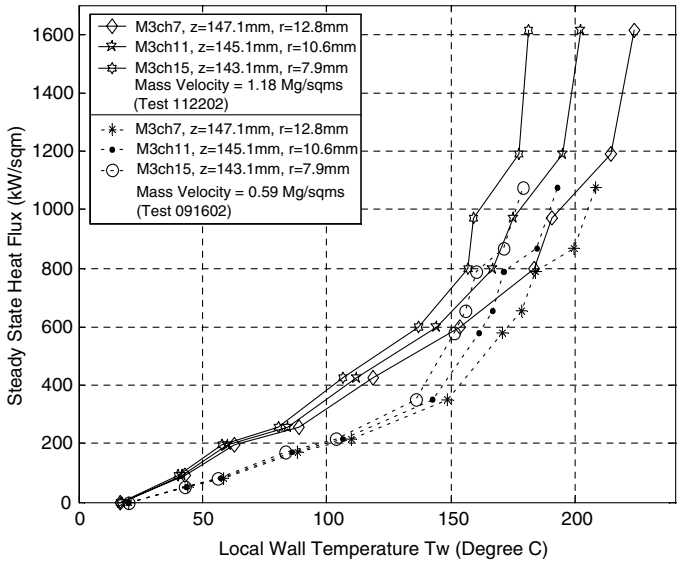

Fig. 6. Steady-state net incident heat flux as a function of the local flow monoblock channel wall temperature at $\phi = 0.0°$ and for specified axial and radial locations (near Z_3) and heaters asymmetrically placed with respect to the axial direction with $L_o = 4.0$ mm and $L_i = 16.0$ mm of unheated flow channel both downstream and upstream of the heaters, respectively.

4. Conclusions

Three-dimensional thermal measurements for a one-side-heated square outside boundary cross-section monoblock (with a circular inside diameter) show: (1) the three-dimensional variation of the wall temperature close to both the heated and fluid/solid surface boundaries, (2) the resultant effects of mass velocity on the three-dimensional wall temperature/outside heat flux relationship, and (3) the occurrence of local CHF and local post-CHF. When expanded, this data will provide a basis for characterizing and correlating the actual three-dimensional conjugate heat transfer in one-side heated monoblocks, plasma-facing-components, and other high-heat flux applications for local post-critical heat flux, local critical heat flux, local two-dimensional turbulent flow boiling, and possibly the global critical heat flux [2].

Acknowledgements

The authors are appreciative to the Department of Energy (DOE) for its support of this work under contract #DEFGO3-97ER54452. The authors are also appreciative to Mrs. Vivian Pope, Mr. Richard J. Martin, and the Thermal Science Research Center personnel for supporting many aspects of this work.

References

[1] R.D. Boyd, P. Cofie, Q.Y. Li, A. Ekhlassi, A new facility for measurements of three-dimensional, Local subcooled flow boiling heat flux and related critical heat flux, in: Proc. of the International Mechanical Engineering Congress and Exposition (IMECE), 5–10 November 2000, HTD-866-4, American Society of Mechanical Engineering, Orlando, FL, 2000, pp. 199–208.

[2] D.L. Youchison, J. Schlosser, F. Escourbiac, K. Ezato, M. Akiba, C.B. Baxi, Round robin CHF testing of an ITER vertical target swirl tube, 18th IEEE/NPSS Symposium on Fusion Engineering, Albuquerque, NM, 1999, pp. 385–387.

[3] M. Akiba, K. Ezato, K. Sato, S. Suzuki, T. Hatano, Development of high heat flux components in JAERI, 18th IEEE/NPSS Symposium on Fusion Engineering, Albuquerque, NM, 1999, pp. 381–384.

[4] D.L. Youchison, R.E. Nygren, S. Griegoriev, D.E., Driemeyer, CHF comparison of an attached-fin hypervapotron and porous-coated channels, 18th IEEE/NPSS Symposium on Fusion Engineering, Albuquerque, NM, 1999, pp. 388–391.

[5] D.L. Youchison, C.H. Cadden, D.E. Driemeyer, G.W. Wille, Evaluation of helical wire inserts for CHF enhancement, 18th IEEE/NPSS Symposium on Fusion Engineering, Albuquerque, NM, 1999, pp. 119–122.

[6] T. Marshall, Experimental examination of the post-critical heat flux and loss of flow accident phenomena for prototypical ITER divertor channels, Ph.D. Thesis, Nuclear Engineering Department, Renesselaer Polytechnic Institute, 1998.

[7] J. Boscary, M. Araki, M. Akiba, Critical heat flux database of JAERI for high heat flux components for fusion applications, JAERI-Data/Code 97-037, Japan Atomic Energy Research Institute, 1997a.

[8] J. Boscary, M. Araki, M. Akiba, Analysis of the JAERI critical heat flux data base for fusion application, JAERI-Data/Code 97-037, Japan Atomic Energy Research Institute, 1997b.

[9] T.D. Marshall, R.D. Watson, J.M. McDonald, D.L. Youchison, Experimental investigation of post-CHF enhancement factor for a prototypical ITER divertor plate with water coolant, Symposium on Fusion Engineering, IEEE, 1995, pp. 206–209.
[10] R. Inasaka, H. Nariari, Critical heat flux of subcooled flow boiling in swirl tubes relevant to high-heat-flux components, Fusion Technol. 29 (1996) 487.
[11] M. Akiba et al., Experiments on heat transfer of smooth and swirl tubes under one-sided heating conditions, presented at the US/Japan Workshop, Q182, on Helium-Cooled High Heat Flux Components Design, General Atomics Corporation, San Diego, CA, 1994.
[12] G.P. Celata, M. Cumo, A. Mariani, A mechanistic model for the prediction of water-subcooled-flow-boiling critical heat flux at high liquid velocity and subcooling, Fusion Technol. 29 (4) (1996) 499.
[13] R.D. Boyd, Similarities and differences between single-side and uniform heating for fusion applications—I: uniform heat flux, Fusion Technol. 25 (1994) 411–418.
[14] M. Araki et al., Experiment on heat transfer of the smooth and the swirl tubes under one-side heating conditions, Department of Fusion Engineering Research, Japan Atomic Energy Research Institute (JAERI) Report, 1994.
[15] K.M. Becker et al., Heat transfer in an evaporator tube with circumferentially non-uniform heating, Int. J. Multiphase Flow 14 (5) (1988) 575–586.
[16] D. Gärtner et al., Turbulent heat transfer in a circular tube with circumferentially varying thermal boundary conditions, Int. J. Heat Mass Transfer 17 (1974) 1003–1018.
[17] R.E. Nygren, Actively cooled plasma facing components for long pulse high power operation, Fusion Eng. Des. 60 (2002) 547–564.
[18] J.G. Collier, Convective Boiling and Condensation, second, McGraw-Hill, New York, 1972, p. 162.